

## Supplementary Materials

# Dynamic Glycan Network Engineering of Native Mucin Enables Reversible, Self-Healing, and Adhesive Hydrogel Interfaces

Yuki Nakamura<sup>a†</sup>, Kanta Numata<sup>a</sup>, Momoka Hirosaki<sup>a</sup>,  
Hiroki Miyajima<sup>a,b</sup> and Satoshi Fujita<sup>a,b,\*</sup>

<sup>a</sup> Department of Frontier Fiber Technology and Science, University of Fukui, 910-8507, Fukui, Japan.

<sup>b</sup> Life Science Innovation Center, University of Fukui, 910-8507, Fukui, Japan.

\*Corresponding author. E-mail: [fujitas@u-fukui.ac.jp](mailto:fujitas@u-fukui.ac.jp)

## Contents

Figure S1	p. 3
Results and Discussion: FTIR Analysis	p. 3
References	p. 4
Figure S2	p. 5
Figure S3	p. 6
Results and Discussion: Measurement of Adhesion Strength	p. 6
Supplementary Movies: Caption (Movie S1-S4)	p. 7

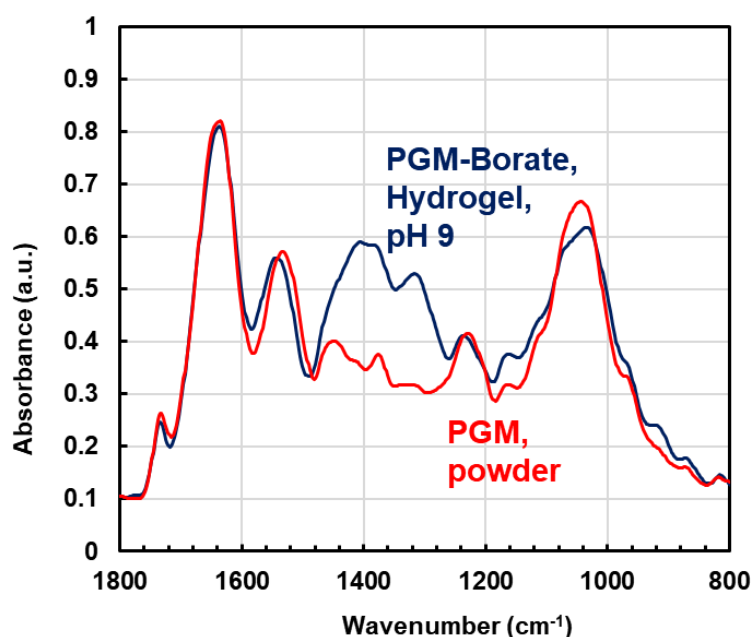


**Figure S1.** FTIR spectra of native PGM powder (red) and the borate-crosslinked PGM hydrogel prepared at pH 9 (blue).

## Results and Discussion

### *FTIR Analysis*

As shown in **Figure S2**, native PGM powder displayed characteristic bands at  $1375\text{ cm}^{-1}$  ( $\text{CH}_3$  bending),  $1448\text{ cm}^{-1}$  ( $\text{CH}_2$  scissoring),  $1533\text{ cm}^{-1}$  (amide II), and  $1635\text{ cm}^{-1}$  (amide I). Upon addition of borate, the spectral pattern changed substantially. The native C–O stretching band at  $1030\text{--}1050\text{ cm}^{-1}$  decreased in intensity, while absorptions increased at  $1180\text{--}1200\text{ cm}^{-1}$ . A strong, broad band developed near  $1310\text{ cm}^{-1}$  and additional broad features appeared in the  $1390\text{--}1410\text{ cm}^{-1}$  region.

These changes correspond to established FTIR signatures of borate–diol complexation. The reduction of the  $1030\text{--}1050\text{ cm}^{-1}$  band indicates consumption of mucin glycan cis-diols during ester formation. The enhanced absorption near  $1310\text{ cm}^{-1}$  matches the tetrahedral  $\text{BO}_4$ -type B–O–C asymmetric stretch reported for PVA–borax and alginate/gelatin–borate hydrogels [1–3], indicating the presence of  $\text{BO}_4$ -coordinated borate species bound to mucin diols. The strong, broad band around  $1400\text{ cm}^{-1}$  aligns with the trigonal  $\text{BO}_3$ -type B–O–C stretch typically observed at  $1409\text{--}1420\text{ cm}^{-1}$  in polymer–borate networks [1,2], confirming  $\text{BO}_3$ -based borate ester formation. The coexistence of  $\text{BO}_3$ - and  $\text{BO}_4$ -associated bands indicates mixed coordination states of borate within the mucin matrix.

Overall, the spectral evolution from 1050 to 1450  $\text{cm}^{-1}$  demonstrates that borate forms reversible PGM–borate crosslinked domains consisting of B–O–C ester linkages and mixed  $\text{BO}_3/\text{BO}_4$  coordination. These signatures parallel those of other polysaccharide–borate hydrogels [1–3], indicating that borate reorganizes the PGM network at the molecular scale.

## References

- [1] Nath, K.; Dave, H. K. Synthesis, Characterization and Application of Disodium Tetraborate Cross-Linked Polyvinyl Alcohol Membranes for Pervaporation Dehydration of Ethylene Glycol. *Acta Chim. Slov.* 2018, **65** (4), 902–918. <https://doi.org/10.17344/acsi.2018.4581>
- [2] Al-Emam, E.; Soenen, H.; Caen, J.; Janssens, K. Characterization of Polyvinyl Alcohol–Borax/Agarose (PVA-B/AG) Double Network Hydrogel Utilized for the Cleaning of Works of Art. *Herit. Sci.* 2020, **8**, 106. <https://doi.org/10.1186/s40494-020-00447-3>
- [3] Verni, E.; Sabatini, F.; Lee, C.; Fiocco, G.; Weththimuni, M. L.; Vigani, B.; Lange, H.; Malagodi, M.; Volpi, F. Development and Characterization of Novel Tannin-Modified Konjac Glucomannan Hydrogels with Optimized Crosslinking Features. *Carbohydr. Polym. Technol. Appl.* 2025, **11**, 100875. <https://doi.org/10.1016/j.carpta.2025.100875>

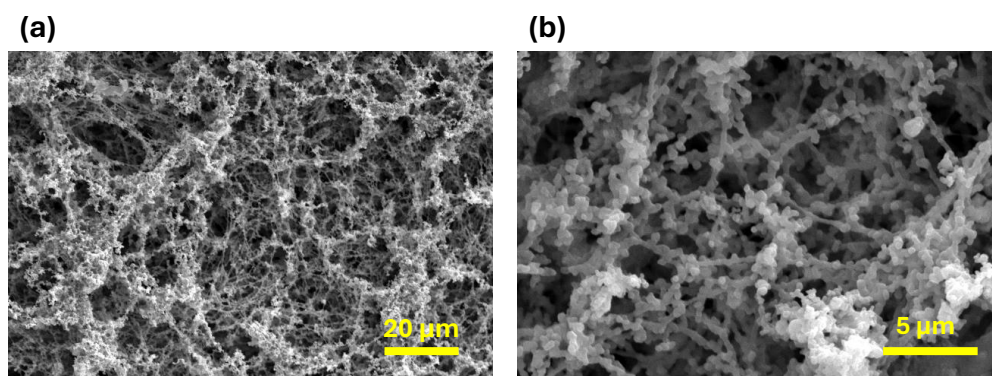


**Figure S2.** SEM images of PGM–borate hydrogel prepared at pH 9. The hydrogel was solvent-exchanged with ethanol in a stepwise manner, followed by t-butyl alcohol, and subsequently freeze-dried. (a) Low magnification. Bar = 20  $\mu\text{m}$ . (b) High magnification. Bar = 5  $\mu\text{m}$ . These images confirm the formation of an interconnected porous network characteristic of borate–crosslinked systems.

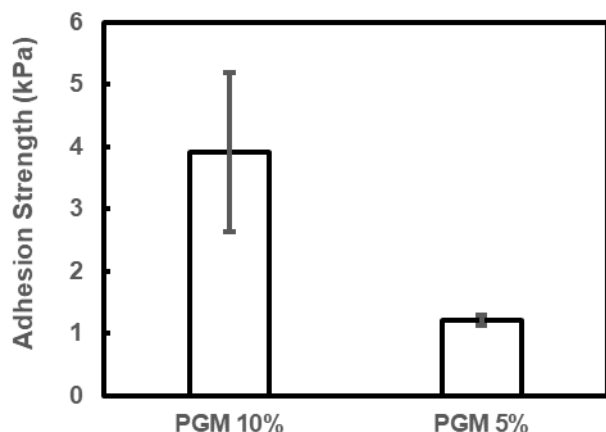


**Figure S3.** Adhesion strength of PGM–borate hydrogels prepared with different PGM concentrations (5% and 10%). Adhesion strength was measured using a universal testing machine by sandwiching the hydrogel between two oxygen-plasma-treated acrylic plates (diameter 3 mm). The applied load at detachment was normalized by the contact area to obtain the adhesion strength (kPa). Bars represent the mean  $\pm$  SD ( $n = 3$ ).

## Results and Discussion

### *Measurement of Adhesion Strength*

As shown in **Figure S3**, the adhesion strength of the PGM–borate hydrogels increased with increasing PGM concentration. The 10% PGM hydrogel showed an adhesion strength of approximately 4 kPa, whereas the 5% PGM hydrogel exhibited values around 1 kPa. This concentration-dependent increase demonstrates that the amount of PGM present in the hydrogel directly influences the measured adhesion strength.

The higher adhesion strength observed at 10% PGM suggests that PGM itself plays a central role in establishing adhesion to the plasma-treated acrylic surface. A greater PGM concentration provides more polymer chains and more borate-binding sites, increasing the number of functional groups capable of interacting with the hydrophilic acrylic surface. The polar glycans in PGM can form hydrogen bonds or other polar interactions with oxygen-containing groups introduced on the acrylic by plasma treatment, promoting stronger interfacial contact. These considerations support the conclusion that PGM contributes directly to the adhesion of the PGM–borate hydrogel to the acrylic substrate.

## Supplementary Movies

**Movie S1** Self-healing behavior of the PGM/BA hydrogel (10% PGM mixed with 300 mM BA, pH 8.0) after a 60 s contact time. Two differently dyed hydrogel pieces were cut and brought into contact, followed by a 60 s healing period. The movie shows the complete self-healing process and the successful stretching of the rejoined gel. This movie corresponds to Fig. 4a.

**Movie S2** Self-healing behavior of the PGM/BA hydrogel after a 10 s contact time. The two cut gel pieces were briefly brought into contact for 10 s. The movie shows partial or insufficient healing, with the interface failing during subsequent handling.

**Movie S3** Self-healing behavior of the PGM/BA hydrogel with 0 s contact time. The cut gel pieces were placed in brief contact without any holding time, resulting in no observable healing. The movie shows immediate separation upon manipulation.

**Movie S4** Adhesive behavior of the PGM/BA hydrogel (10% PGM mixed with 300 mM BA, pH 8.0). A hydrogel sample placed on a glass plate was pressed against the bottom of a glass beaker for 10 s. The movie shows the attachment process and the lifting of the glass plate by holding the adhered beaker. This movie corresponds to Fig. 4b.